IOPscience iopscience.iop.org

Home Search Collections Journals About Contact us My IOPscience

Spin-glass ordering in a spinel ferrite, $Mg(Al, Fe)_2O_4$

This article has been downloaded from IOPscience. Please scroll down to see the full text article.

2000 J. Phys.: Condens. Matter 12 9667

(http://iopscience.iop.org/0953-8984/12/46/314)

View the table of contents for this issue, or go to the journal homepage for more

Download details:
IP Address: 171.66.16.221
The article was downloaded on 16/05/2010 at 07:00

Please note that terms and conditions apply.

J. Phys.: Condens. Matter **12** (2000) 9667–9687. Printed in the UK PII: S0953-8984(00)15114-8

Spin-glass ordering in a spinel ferrite, $Mg(Al, Fe)_2O_4$

S C Bhargava†, A H Morrish, H Kunkel and Z W Li
Department of Physics, University of Manitoba, Winnipeg, Manitoba, Canada, R3T 2N2

Received 3 July 2000, in final form 4 October 2000

Abstract. Non-linear susceptibility (χ_{nl}) measurements on $MgAl_{1.4}Fe_{0.6}O_4$ show spin-glass ordering in a cubic spinel ferrite, for the first time. The ordering gives a peak in the temperature dependence of χ_{nl}, which shows that the spin ordering is a cooperative phase transition. The values of the critical exponents, obtained from χ_{nl} as the temperature approaches the transition temperature, are found to lie in the range obtained from measurements on other spin glasses. We also investigate the static and dynamical effects of the spin-glass ordering on Mössbauer spectra. Dynamical spin freezing as a result of spin-glass ordering is observable in Mössbauer spectra.

1. Introduction

The effects of randomness and frustration on the magnetic properties of a mixed ferrite are remarkable. Cations in a ferrite occupy one of the two inequivalent types of site, known as A and B sites, respectively. The distribution of the diamagnetic and magnetic cations on either of the two types of site is random. This magnetic disorder and the short-range nature of the magnetic interactions have been found to be responsible for the low values of the single-ion spin relaxation rates [1–7]. Frustration is present because both the interactions, the inter-sublattice (J_{AB}) and the intra-sublattice (J_{AA} and J_{BB}) interactions, are antiferromagnetic. When $J_{AB} \gg J_{AA}$, J_{BB}, ferrimagnetic ordering appears in which A and B magnetic sublattices are anti-parallel. In this case, J_{AB} is satisfied but J_{AA}, J_{BB} remain frustrated. When the magnetic ions are substituted for with diamagnetic cations, the inter-sublattice interaction becomes weaker. When it becomes comparable to the intra-sublattice interaction, the A and B sublattices no longer remain anti-parallel, but become non-collinear [8–14]. The localized canting model of the non-collinear spin structure provides a good description of the variation of non-collinearity from site to site due to the randomness and frustration, particularly when the diamagnetic cations occur on both types of inequivalent site [15]. The model shows that the non-collinearity can occur simultaneously at both types of site, varies from site to site, and can become larger than 90° when most of the neighbouring sites are occupied by diamagnetic cations. Eventually, at larger concentrations of the diamagnetic cations, non-collinearity angles greater than 90° are frequently found. In this case, the spin arrangement resembles spin-glass ordering. It is interesting to investigate whether such an oxide shows characteristics of a canonical metallic spin glass, even though the natures of magnetic interactions in an oxide and a metallic substance are quite different.

In a spin glass [16–19], the direction of the moment changes from site to site, but, unlike in a paramagnet, remains unchanged at any site. The spin-glass ordering is characterized by the appearance of a sharp cusp in the temperature dependence of the low-field AC susceptibility.

† Present address: Solid State Physics Division, Bhabha Atomic Research Centre, Bombay 400094, India.

0953-8984/00/469667+21$30.00 © 2000 IOP Publishing Ltd

The peak at the ordering temperature (T_{sg}) gets smeared and shifts to lower temperatures as the applied DC field increases [20]. The ordering temperature depends on the frequency of the AC field also. Another characteristic found is the large increase in the relaxation time as the temperature decreases. This shows that the spin-glass ordering results in a freezing of the spins [16–19] as the temperature decreases. The temperature dependence of the DC magnetization above T_{sg} shows that the spins are independent only when the temperature is greater than 5 T_{sg}. As the temperature decreases, short-range ordering develops [21, 22]. The size of these regions grow as the temperature approaches T_{sg}. Eventually, long-range spin-glass ordering appears at T_{sg}. Below T_{sg}, there is a branching of the field-cooled (FC) and the zero-field-cooled (ZFC) magnetizations [23–25]. Remanent magnetizations (IRM and TRM) show [16–19] time dependencies. Study of the non-linear susceptibility (χ_{nl}) reveals the nature of the spin-glass transition. The divergence of χ_{nl} at T_{sg} shows that the spin-glass ordering is a true thermodynamic phase transition [26–29]. The critical exponents associated with the transition have been found to vary from substance to substance. Extensive measurements have also been made on the re-entrant spin glasses in earlier studies [30, 31]. In these materials, a paramagnetic-to-ferromagnetic/ferrimagnetic transition occurs as the temperature decreases, at T_P. Subsequently, at a lower temperature, a ferromagnetic-to-spin-glass transition occurs. In the non-linear AC susceptibility, the paramagnetic-to-ferromagnetic transition is characterized by a sharp rise at T_P. It is followed by a plateau and a decrease below T_{sg}. The critical exponents related to T_P show no variation from substance to substance and, thus, show a universal character. The critical behaviour at the spin-glass transition is studied by approaching T_{sg} from lower temperatures. It has been found in earlier studies of the paramagnetic-to-spin-glass transition that χ_{nl} is nearly symmetric about T_{sg}. Thus, it is possible to approach T_{sg} from lower temperatures to study the critical exponents in the re-entrant spin glasses. This gives the advantage that the domain wall motion in the ferromagnetic phase of the re-entrant system does not affect the critical exponents. Until 1998, the re-entrant systems studied were ferromagnet based. In 1998, Tobo and Ito [31] studied an antiferromagnet-based re-entrant system for the first time using χ_{nl} and found the critical exponents associated with the phase transition.

In the earlier studies of the mixed ferrites, AC susceptibility was found [23–25] to show a broad peak and FC and ZFC magnetizations showed branching, even when the spin-glass ordering was not expected and the neutron diffraction method clearly showed the presence of long-range ordering. The broadness of the peak shows that it is not a phase transition. Subsequently, it was shown [6] that these characteristics of the magnetizations resulted from superparamagnetic effects. Nevertheless, the possibility that the mixed oxides can show spin-glass ordering when the randomness and frustration in magnetic interactions are strong remains [32–35]. Predictions have been made of the concentration regions of the mixed ferrites in which spin-glass ordering is expected [33]. As superparamagnetic effects are always present in mixed oxides, there is a need to use a method, like non-linear susceptibility measurement, which can distinguish between superparamagnetism and spin-glass ordering. χ_{nl} shows divergence at the spin-glass ordering temperature, but is not affected by superparamagnetic fluctuations [18, 19]. In the present study, we have investigated $MgAl_{1.4}Fe_{0.6}O_4$, a composition of the mixed ferrite that was predicted to be a spin glass. χ_{nl} unambiguously shows the presence of a spin-glass transition and confirms that the ordering is a thermodynamic phase transition. We find that the critical exponents associated with the transition fall in the range [26, 29, 31] found using other spin glasses. We also see the effects in χ_{nl} which are probably related to the development of short-range order [21, 22] in the temperature range from T_{sg} to 5 T_{sg}. The linear susceptibility also shows a peak, which gets rapidly suppressed and moves to lower temperatures as the applied DC field increases, as is found for canonical metallic spin glasses.

Mössbauer spectroscopy is used to study the static and the dynamic effects of the spin-glass ordering on the Mössbauer spectra. It is interesting to determine the characteristics that can be used to identify the presence of the spin-glass ordering using Mössbauer spectroscopy. The interpretation of the Mössbauer spectrum of the mixed ferrites is, however, very complicated. Earlier studies revealed the presence of a variety of fluctuation processes in the mixed ferrites which affect the Mössbauer spectrum and must be taken into consideration while analysing the complex Mössbauer spectrum. Single-ion spin relaxation affects the spectral shapes at all temperatures, including low temperatures. The randomness in the distribution of magnetic cations and the short-range nature of the magnetic interactions are responsible for the low single-ion spin relaxation rates. This mode of fluctuation is weakly dependent on the temperature and the magnetic field. At higher temperatures, superparamagnetism has been found to affect the Mössbauer spectrum. Even though the crystallite size is not small, the presence of diamagnetic cations causes the magnetic lattice to break into weakly coupled magnetic clusters, which fluctuate independently at higher temperatures. This mode of fluctuation is strongly dependent on the temperature and the magnetic field. The effect of superparamagnetism, in the presence of a variation in the size of clusters, is seen through the appearance of a paramagnetic component coexisting with a magnetic component, with little effect of superparamagnetic fluctuations. The relative intensity of the paramagnetic component increases with temperature. At temperatures greater than 300 K, the effects of the spin–lattice relaxation are observable [36] if the magnetic splitting is present in the Mössbauer spectrum. This mode of fluctuation is not important in the present study. While the single-ion spin relaxation and superparamagnetic fluctuations can be taken into consideration, the effects of freezing due to spin-glass ordering cannot be included unless the precise mechanism of the spin freezing becomes known. Its presence is indirectly seen through its influence on certain parameters, which enter in the calculation of the single-ion spin-relaxation spectra. The analysis of the Mössbauer spectra in the presence of an applied field is far more complicated, due to the uncertain alignment effects of the external field on the spin-glass ordering and the time-dependent effects below T_{sg}.

In an earlier Mössbauer study of the mixed ferrite $Ni_{0.75}Zn_{0.25}Fe_2O_4$, the temperature dependence of $\langle S_Z \rangle$ of Fe^{3+} ions was found [5, 12] to be anomalous. As the temperature increases, the magnetization decreases rapidly initially and slowly above a certain temperature, showing a kink in the temperature dependence of $\langle S_Z \rangle$. Subsequently, the kink in the temperature dependence of $\langle S_Z \rangle$ was found in other studies of the mixed ferrites also [37–40]. It has been shown that the rapid decrease in $\langle S_Z \rangle$ at lower temperatures is due to the presence of non-collinearity. At higher temperatures, the non-collinearity disappears, and $\langle S_Z \rangle$ starts decreasing slowly. On the basis of the anomalous shape of the temperature dependence of $\langle S_Z \rangle$ found using Mössbauer spectroscopy, it was concluded in an earlier study by de Bakker *et al* [40] that $Mg_{1-x}Zn_xFe_{1.5}Cr_{0.5}O_4$ and $MgFe_{2-x}Cr_xO_4$ show spin-glass ordering for certain ranges of x. While their conclusions are likely to be correct, they have not provided direct evidence for the presence of spin-glass ordering. A direct relation between the kink in the temperature dependence of $\langle S_Z \rangle$ and the spin-glass ordering is not known.

In the present study, we have obtained Mössbauer spectra in zero field as well as in the presence of an applied field of 5 T, to study the effects of the spin-glass ordering on Mössbauer spectra. The zero-field spectra show the effects of single-ion spin relaxation even at 4.2 K, and the effects of superparamagnetism at higher temperatures. The superparamagnetic effects are confined to temperatures lower than 20 K, whereas the susceptibility shows the peak due to the spin-glass ordering at temperatures higher than 30 K. Thus, the two effects occur in different regions of temperatures, and the susceptibility peak is not related to superparamagnetism. The analysis of the spectra made in the present study takes into consideration the presence of

single-ion spin relaxation and superparamagnetism. The analyses of spectra obtained with an applied field reveal the presence of additional modes of relaxation, which appear to be related to spin-glass freezing.

2. Experimental details and results

2.1. Linear AC susceptibility

$MgAl_{1.4}Fe_{0.6}O_4$, prepared using the conventional ceramic procedure, was found to be a single-phase cubic spinel. The AC susceptibility was obtained using an AC exciting field of 0.03 Oe rms at a frequency of 300 Hz and a DC biasing field. The measurements were made using three DC fields of 0, 100, and 500 Oe (figure 1). The peak at ≈34 K in zero DC field shifts to lower temperatures and its amplitude decreases as the DC field increases. This is a characteristic of the spin-glass transition. A small broad hump is superimposed on the zero-field AC susceptibility on the higher-temperature side of the main peak. The hump decreases rapidly as the DC field increases and disappears at a field lower than 500 Oe. The origin of this hump is not revealed by the Mössbauer spectroscopy, as there is no visible magnetic component in the spectrum at these higher temperatures. Such a hump at higher temperatures, which is easily suppressed by the DC field, is very prominent in the susceptibility of (Co, Cr)Fe_2O_4. The hump is relatively weak in the zero-field AC susceptibility of $MgAl_{1.4}Fe_{0.6}O_4$. Its presence is, however, clearly seen in the temperature dependence of the non-linear part of the susceptibility, as we will see below, which further highlights the significance of the non-linear susceptibility measurements. The data in the temperature range from 70 to 294 K were fitted with the Curie–Weiss law. In all three fields, the paramagnetic Curie temperature (θ) is found to be ≈250 K. The value of $\theta/T_{sg} \approx 250/34$ is found to be large. This ratio is a measure of the degree of frustration. A higher ratio implies greater frustration, and this results in the spin-glass ordering [41].

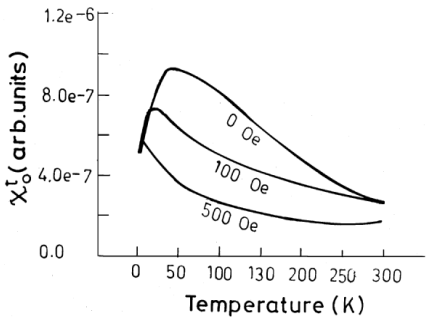

Figure 1. The temperature dependencies of the linear AC susceptibility of $MgAl_{1.4}Fe_{0.6}O_4$ obtained using a driving field of 0.03 Oe (rms) at a frequency of 300 Hz and DC static fields of 0, 100, and 500 Oe.

2.2. Non-linear AC susceptibility

Earlier studies of the mixed ferrites have shown that a peak in the linear AC susceptibility appears due to superparamagnetism also. Thus, this peak is not considered sufficient evidence for the presence of spin-glass ordering. The non-linear part of the susceptibility, on the other hand, shows no peak due to superparamagnetism, but shows a divergent behaviour at the spin-glass ordering temperature [18, 19]. It further shows that the spin-glass ordering is a

thermodynamic phase transition. We, therefore, measured the non-linear susceptibility of the sample under study.

In the presence of a magnetic field h, the magnetization (m) is given by the series [29]

$$m = \chi_0 h + \chi_2 h^3 + \chi_4 h^5 + \cdots. \tag{1}$$

For a driving AC field $h = h_0 \sin \omega t$, the induced signal in the AC-susceptibility measurement is given by

$$\begin{aligned} E &= -nAf(\mathrm{d}m/\mathrm{d}t) \\ &= -nAfh_0[\chi_0^t \cos \omega t - (3/4)h_0^2\chi_2^t \cos 3\omega t + (5/16)h_0^4\chi_4^t \cos 5\omega t + \cdots]. \end{aligned} \tag{2}$$

Here, n is the number of turns per unit length, A is the cross-sectional area of the pick-up coil, f is the filling factor, and

$$\begin{aligned} &\chi_0^t = \chi_0 + (3/4)h_0^2\chi_2 + (5/8)h_0^4\chi_4 + \cdots \\ &\chi_2^t = \chi_2 + (5/4)h_0^2\chi_4 + \cdots \\ &\chi_4^t = \chi_4 + (7/4)h_0^2\chi_6 + \cdots \\ &\text{etc.} \end{aligned}$$

If higher non-linear terms are neglected,

$$\begin{aligned} &\chi_0 \approx \chi_0^t \\ &\chi_2 \approx \chi_2^t \\ &\chi_4 \approx \chi_4^t \\ &\text{etc.} \end{aligned}$$

When a DC field h_{dc} (like the remanent field of the superconducting magnet) is present in addition to the driving field, i.e. $h = h_{dc} + h_0 \sin \omega t$, the induced signal in the AC susceptibility measurement can be shown to be

$$\begin{aligned} E = -nAfh_0[&\chi_0^t \cos \omega t + 3\chi_1^t h_0 \sin 2\omega t - (3/4)h_0^2\chi_2^t \cos 3\omega t \\ &- (5/2)h_0^3\chi_3^t \sin 4\omega t + (5/16)h_0^4\chi_4^t \cos 5\omega t + \cdots] \end{aligned} \tag{3}$$

where

$$\begin{aligned} &\chi_0^t = \chi_0 + [(3/4)h_0^2 + 3h_{dc}^2]\chi_2 + [5h_{dc}^4 + (15/2)h_{dc}^2h_0^2 + (5/8)h_0^4]\chi_4 + \cdots \\ &\chi_1^t = h_{dc}\chi_2 + (1/3)[10h_{dc}^3 + 5h_0^2h_{dc}]\chi_4 + \cdots \\ &\chi_2^t = \chi_2 + [(5/4)h_0^2 + 10h_{dc}^2]\chi_4 + \cdots \\ &\chi_3^t = \chi_4 h_{dc} + [\cdots]\chi_6 \\ &\chi_4^t = \chi_4 + [(7/4)h_0^2 + \cdots]\chi_6 + \cdots. \end{aligned}$$

If higher non-linear terms are neglected,

$$\begin{aligned} &\chi_0^t \approx \chi_0 \\ &\chi_1^t \approx h_{dc}\chi_2 \\ &\chi_2^t \approx \chi_2 \\ &\chi_3^t \approx h_{dc}\chi_4 \\ &\chi_4^t \approx \chi_4. \end{aligned}$$

In the presence of the DC field h_{dc}, the coefficients of the 2ω, 4ω, etc, terms (χ_1^t, χ_3^t, etc) are also finite. These non-zero even harmonics (χ_1^t, χ_3^t, etc) depend on h_{dc}, and indicate temperature dependencies of only the higher odd harmonics (χ_2^t, χ_4^t, etc, respectively) are

significant. It may be noted that all of the terms in E contain only odd powers of the magnetic field, even though χ_1^t, χ_3^t, etc are finite, as is desired. The temperature dependencies of the odd harmonics are not affected by the presence of h_{dc}. Experimentally, we minimize the even harmonics at a temperature where the maxima in χ_2^t, χ_4^t, etc are expected by applying a DC field, to compensate the remanent field of the superconducting magnet. In the following, we discuss the temperature dependencies of the odd harmonics only. Using an AC susceptometer (QUANTUM DESIGN PPMS Model 6000), we measure the temperature dependencies of the coefficients of the ωt, $3\omega t$, $5\omega t$ terms in equation (3), using $h_0 = 16$ Oe, $f = 300$ Hz, and $h_{dc} \approx 0$ Oe. These quantities are denoted as M, M_3, and M_5, respectively. They give the temperature dependencies of χ_0^t, χ_2^t, and χ_4^t, respectively.

Before making measurements on the ferrite sample under investigation, we made measurements on a well known canonical spin glass Pd–5.5 at.% Mn, which undergoes spin-glass ordering at 3.1 K. We observed divergence in the non-linear susceptibility, as expected. This made us confident of the capability of our instrument. Minor smearing of the divergence is found. This is due to the larger frequency of the driving field used and the dynamic nature of our measurement. The temperature was continuously changed at the rate of 1 °C per five minutes. The ferrite under investigation is an insulator in the form of a cylinder of diameter 5 mm and height 5 mm. Even though the sample is in a helium atmosphere and the temperature is raised slowly, the temperature within the sample may not be uniform, which could result in appreciable smearing of the divergence.

The temperature dependencies of M_3 and M_5 are shown in figure 2. Two peaks in the temperature dependencies of the third and fifth harmonics are visible. The cause of the peak

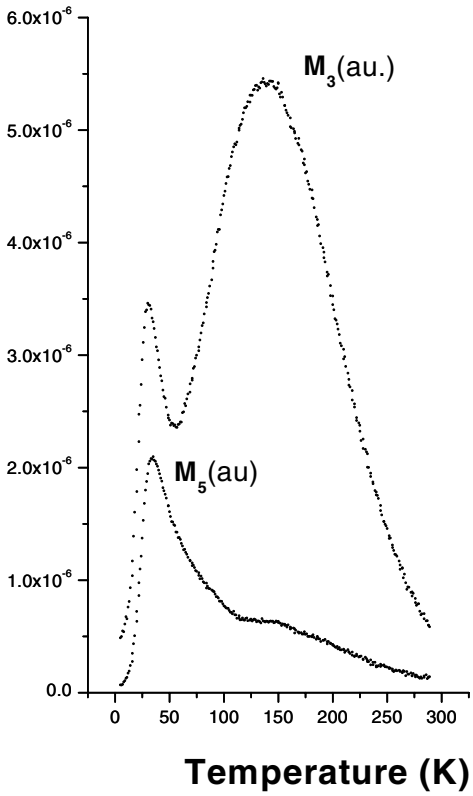

Figure 2. The temperature dependencies of M_3 and M_5 obtained using a field $h = h_{dc} + h_0 \sin \omega t$, where $h_{dc} = 0$ Oe, $h_0 = 16$ Oe, and $f = 300$ Hz.

at the higher temperature is not clear to us at this time. Mössbauer spectra show an absence of magnetic long-range ordering at these higher temperatures even in an applied field of 5 T. It appears that the short-range order which appears in the spin glasses in the temperature range from T_{sg} to 5 T_{sg} may be responsible for the higher-temperature peak. The dependence of M_3 on $t = |(T - T_{sg})/T_{sg}|$ is plotted on double logarithmic scales for temperatures lower than T_{sg} in figure 3. The slope is found to be 1.52. The dependence of M_5 on $|(T - T_{sg})/T_{sg}|$ is also plotted on double logarithmic scales for temperatures lower than 34 K in figure 3. The slope is found to be 3.56. The double logarithmic plots flatten as $t \to 0$ in figure 3.

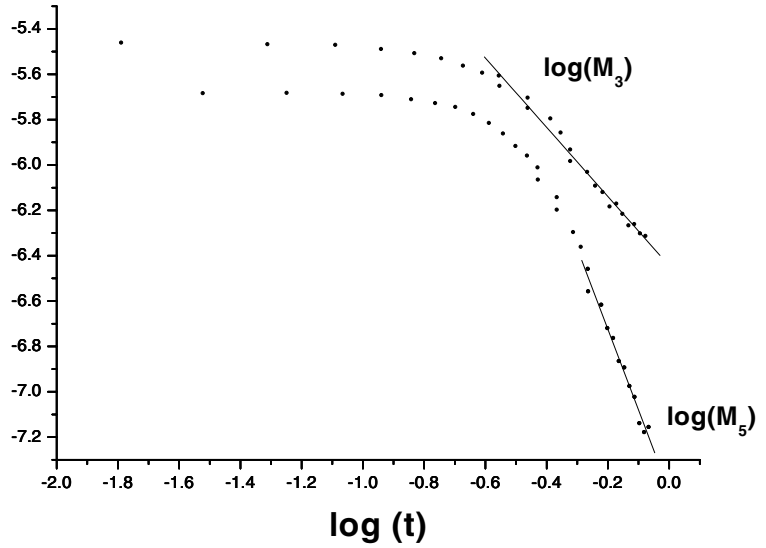

Figure 3. Double logarithmic plots of M_3 and M_5 as functions of the reduced temperature t at $T < T_{sg}$.

2.3. Mössbauer spectroscopy

Mössbauer measurements have been made using a cryogenic device (Oxford Model A26322) and a ^{57}Co-in-Rh Mössbauer source of strength 50 mCi. Temperature control was achieved using a temperature controller (Lake Shore) and a capacitance thermometer. Temperature measurements were made with a Rh–Fe resistance sensor. A sine wave was used to drive the spectrometer. The velocity scale was linearized before the analysis of the data was carried out.

Mössbauer spectra in zero field are shown in figures 4(a) and 4(b). Effects of the single-ion spin relaxation are visible even at 4.2 K. Superparamagnetic effects appear at higher temperatures. This is shown by the gradual conversion of the magnetic spectrum into a paramagnetic spectrum as the temperature increases. Superparamagnetic effects are confined to temperatures lower than 20 K. The spectra of $MgAl_{1.4}Fe_{0.6}O_4$ in the presence of a longitudinal field of 5 T are shown in figures 5(a) and 5(b). There is no partial conversion of the magnetic spectrum into a paramagnetic spectrum with the increase in temperature. This is due to the suppression of the superparamagnetic fluctuations by the applied field. As a result, the magnetic splitting in the Mössbauer spectrum is observable even at temperatures higher than 25 K. The decrease in the line broadening with temperature at the lower temperatures in these spectra (figure 5) is remarkable. It is partly due to the freezing of spins as the temperature decreases.

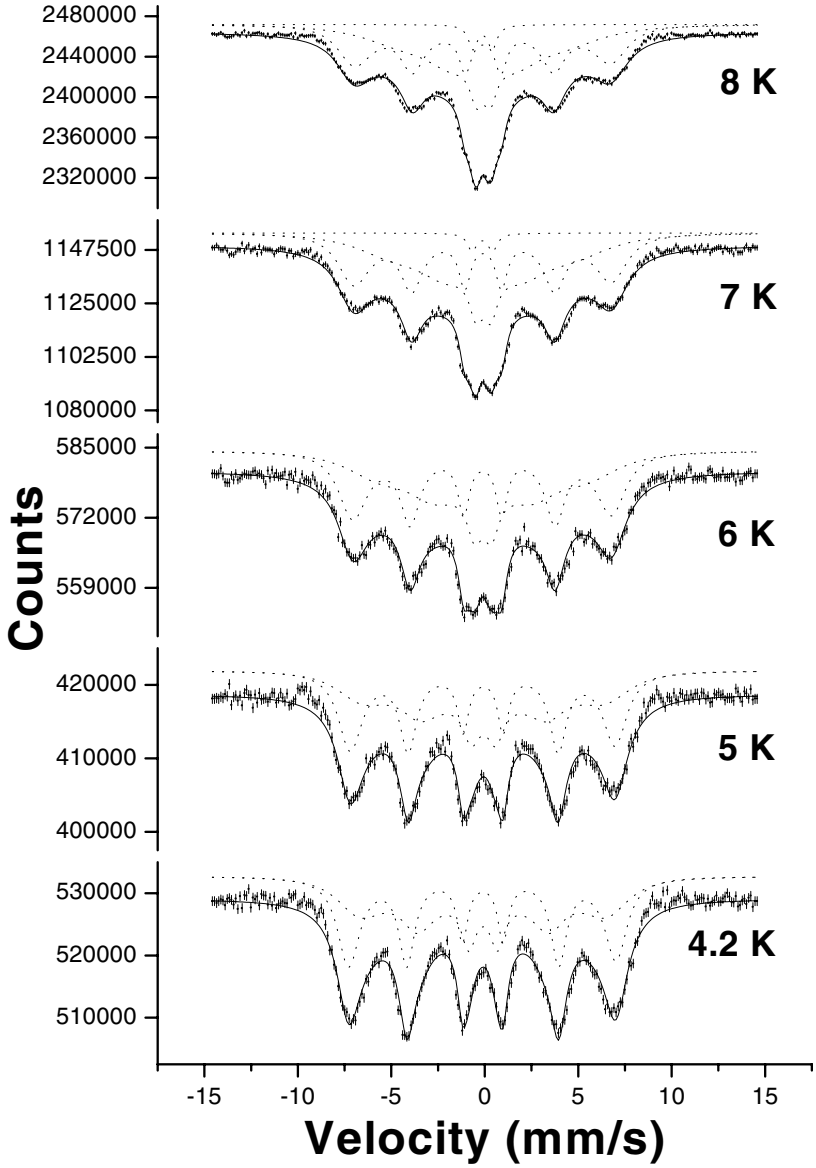

(a)

Figure 4. (a), (b) Mössbauer spectra of $MgAl_{1.4}Fe_{0.6}O_4$ in the absence of an applied magnetic field. Solid lines show the theoretical relaxation spectra which best fit the experimental spectra. The component spectra are shown by dotted lines.

2.3.1. Cation distribution. Cations in a ferrite occupy tetrahedral (A) and octahedral (B) sites. To determine the preferences of Fe for the two inequivalent sites, the paramagnetic spectrum at 30 K in zero field is fitted with two symmetric doublets. The results of the analysis are given in table 1. By using an earlier result that $\delta_A < \delta_B$ and $\epsilon_A < \epsilon_B$, where δ and ϵ represent the centre shift and the quadrupole splitting, respectively, we can conclude that the first component in table 1 originates from the A site and the second component originates from the B site. Thus, the

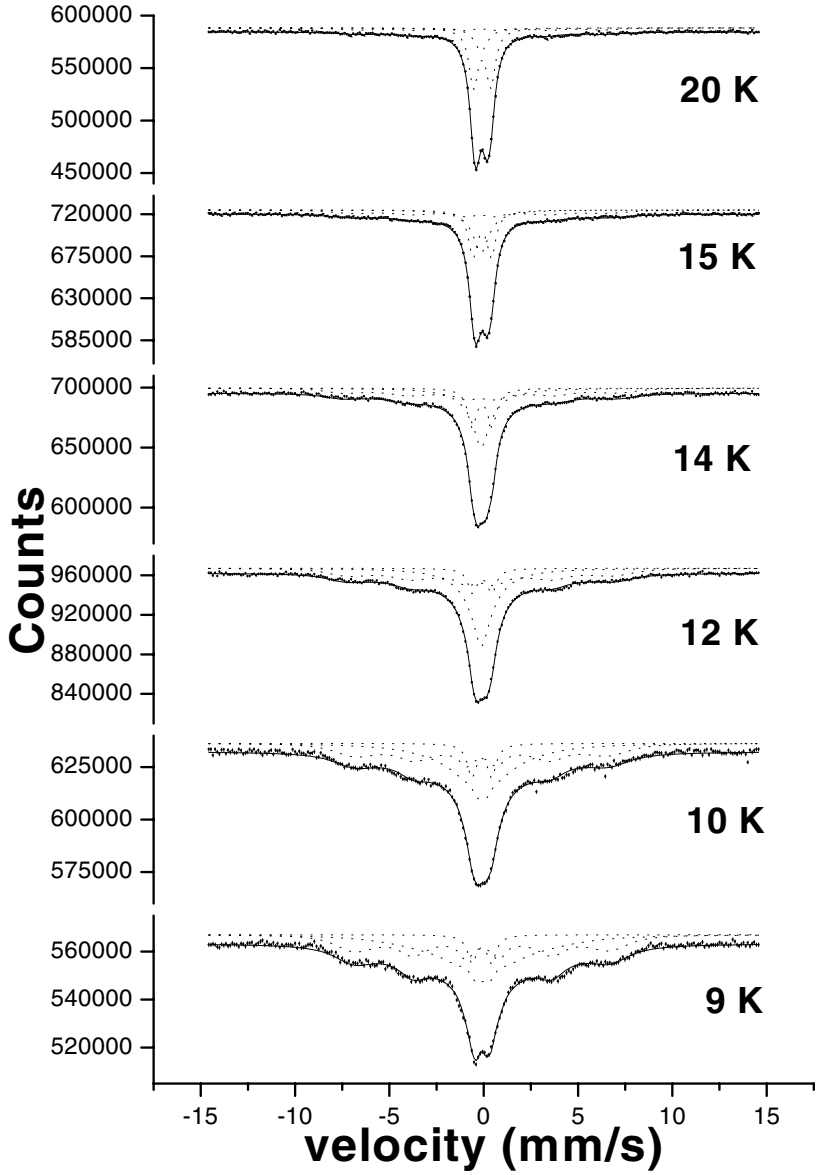

(b)

Figure 4. (Continued)

cation distribution is concluded to be $[(Mg, Al)_{0.7}Fe_{0.3}]_A[(Mg, Al)_{1.7}Fe_{0.3}]_BO_4$. On referring to figure 8 of reference [33], we find that $C_A = 0.3$ and $C_B = 0.15$. Here, C_A and C_B refer to the fraction of A and B sites occupied by Fe ions. This lies in the spin-glass region of the phase diagram (figure 8 of reference [33]).

2.3.2. Spin-glass ordering. The effects of an applied field on the Mössbauer spectrum can be seen visually by comparing the spectra at low temperatures where the relaxation broadening is

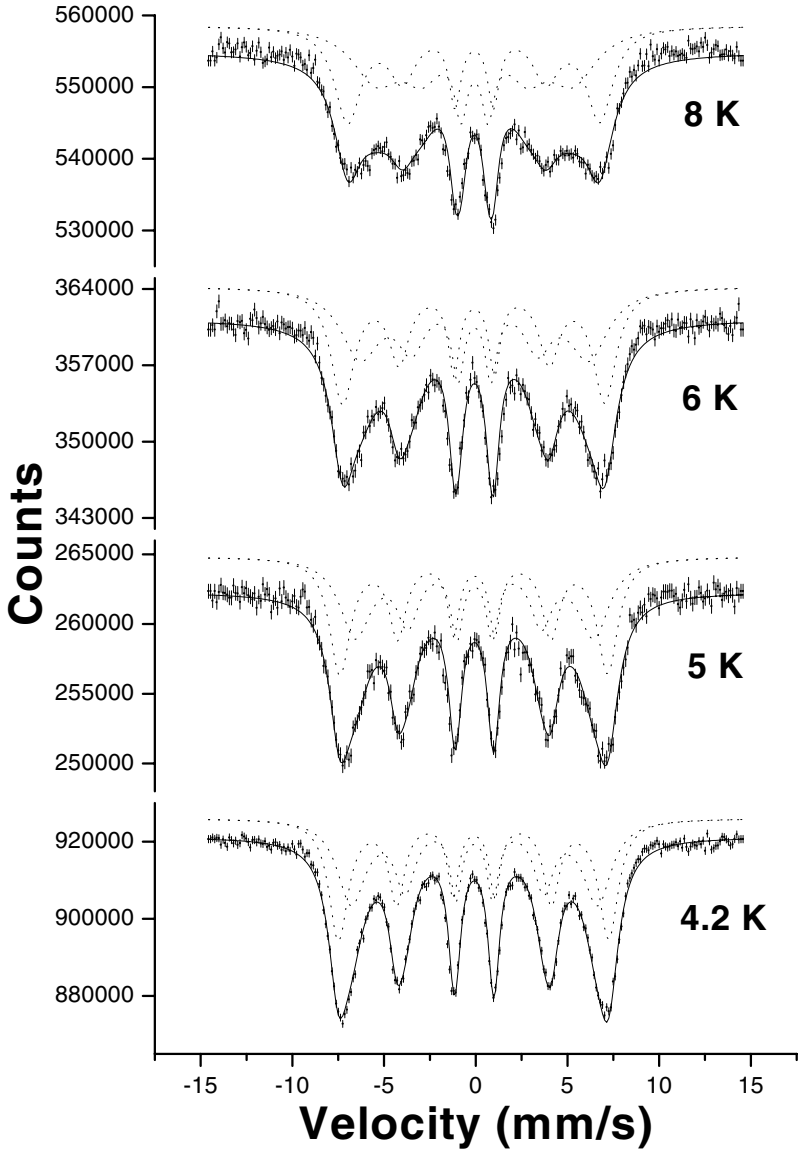

(a)

Figure 5. (a), (b) Mössbauer spectra of $MgAl_{1.4}Fe_{0.6}O_4$ in the presence of an applied magnetic field of 5 T. Solid lines show the theoretical relaxation spectra which best fit the experimental spectra. The component spectra are shown by dotted lines.

small. The spectrum in the absence of an applied field shows appreciable relaxation broadening even at 4.2 K. We, therefore, obtained a spectrum at 1.8 K where the relaxation broadening is small. In the presence of the applied field of 5 T, the relaxation broadening gets suppressed. Consequently, the spectrum at 4.2 K in the presence of the applied field has insignificant relaxation broadening. In view of this, and the difficulty in recording a spectrum at 1.8 K in the presence of an applied field, we did not make measurements in the presence of the applied field at lower temperatures. The spectra at 1.8 K in zero field and 4.2 K in the presence of the

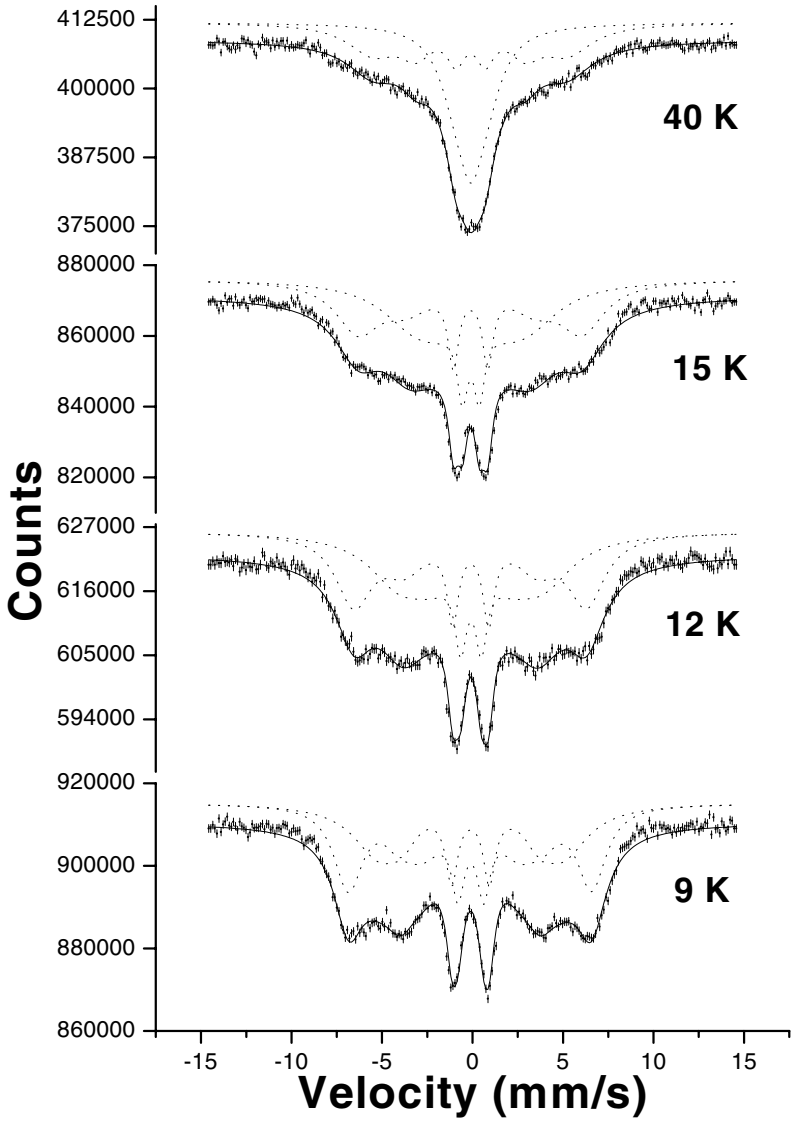

(b)

Figure 5. (Continued)

Table 1. Results of the analysis of the paramagnetic spectrum at 30 K, obtained in the absence of an applied field. (RI stands for relative intensity.)

Component 1 A site				Component 2 B site			
ϵ (mm s^{-1})	δ (mm s^{-1})	Γ (mm s^{-1})	RI (%)	ϵ (mm s^{-1})	δ (mm s^{-1})	Γ (mm s^{-1})	RI (%)
0.46	0.16	0.49	49.7	0.89	0.20	0.5	50.3

applied field of 5 T are fitted using simple sextets to estimate the effect of the applied field. The two spectra are compared in table 2.

Table 2. Results of analyses of magnetic spectra at low temperatures, fitted with simple sextets.

4.2 K, 50 kOe				1.8 K, 0 kOe			
H_{int} (kOe)	δ (mm s^{-1})	$\epsilon(M)$ (mm s^{-1})	I_{16}:I_{25}:I_{34}	H_{int} (kOe)	δ (mm s^{-1})	$\epsilon(M)$ (mm s^{-1})	I_{16}:I_{25}:I_{34}
446.6	0.21	−0.08	2.46:1.57:1.0	452.7	0.19	0.04	2.64:1.84:1.0

We observe the following effects of the applied field (table 2). Firstly, the lines do not split. Secondly, the difference between the fields characterizing the spectra in the two fields appears to be due to the difference in the temperature of measurement only. The applied field does not affect the hyperfine field directly. Finally, the changes in the relative intensities of the three pairs of lines of the sextet, as a result of the application of the applied field, are small. As will be discussed later, these three effects also show the presence of spin-glass ordering. As the applied field is large, a small alignment of the spins by the applied field is not unexpected and is in fact observed. Nevertheless, the effect of the applied field on the Mössbauer spectrum clearly indicates the presence of spin-glass ordering at lower fields.

2.3.3. Analyses of Mössbauer spectra. In earlier studies of the mixed ferrites which show non-collinear spin ordering as well as superparamagnetism, but not the spin-glass ordering, Mössbauer spectra were satisfactorily interpreted by taking into consideration the presence of single-ion spin relaxation as well as superparamagnetism. We will attempt to analyse the Mössbauer spectra of the oxide under study also using the same procedure, even though we expect additional effects due to the spin-glass ordering and spin freezing. The additional effects are prominent in the spectra obtained in the presence of an applied field which can be seen even from a visual inspection of the spectra. Specifically, the lines are found to be broader than is expected on the basis of single-ion spin relaxation or superparamagnetism even at lower temperatures. We think that this characteristic of the Mössbauer spectrum can be used to identify the presence of spin-glass ordering in these oxides.

The formalisms appropriate for single-ion spin relaxation and collective fluctuations are different. In single-ion spin relaxation, the six ionic states of the Fe^{3+} ion are involved. A minimum of a 6×6 matrix describes the relaxation process. In the case of collective fluctuations such as superparamagnetic fluctuation between two states, a 2×2 matrix describes the relaxation process. The presences of the two types of fluctuation cannot be simultaneously included in the line-shape formula. However, a simplification is available for treating superparamagnetism when there is a distribution in particle size.

Superparamagnetic fluctuations convert a magnetic spectrum into a paramagnetic spectrum. In view of the exponential dependence of the relaxation frequency on the temperature, this conversion occurs in a very narrow range of temperature if the particle size is uniform. When there is a large variation in the cluster sizes, there are three components in the spectrum at any temperature. There is a fraction of the spectrum that is under the influence of superparamagnetic fluctuation and also shows magnetic splitting. At any temperature, this fraction (we call it I_2) is small. There is also a part corresponding to larger clusters which is not yet under the influence of superparamagnetic fluctuation (we call it I_1). The third part of the spectrum corresponds to smaller clusters, and becomes a paramagnetic spectrum at lower temperatures (we call it I_3). At any temperature, the relative intensity of I_2 is small and can be neglected in the analyses when there is a large variation in the cluster size. In other words, to a good approximation, the Mössbauer spectrum can be fitted with a magnetic component showing the effects of single-ion spin relaxation only, with no effect of superparamagnetism,

corresponding to I_1, and a paramagnetic component corresponding to I_3.

The theoretical spectrum for fitting the magnetic component I_1 is computed using the stochastic model of single-ion spin relaxation [42], described elsewhere [43, 44]. The spectral shape corresponding to a nuclear transition is given by [2, 3, 43, 44]

$$I(\omega) = \left(\frac{2}{\Gamma}\right) \mathrm{Re} \sum_{\alpha=1}^{6} \mathrm{i} \frac{q_\alpha}{\omega - p_\alpha}. \tag{4}$$

Here, the summation is over the six ionic states of the Fe^{3+} ion, Γ is the full width at half-maximum in the absence of relaxation effects, and p_α are the eigenvalues of the (6×6) matrix **P** with elements

$$P_{\mu\mu'} = \left[\left(\omega^\mu - \frac{1}{2}\mathrm{i}\Gamma\right)\delta_{\mu\mu'} + \mathrm{i}W_{\mu\mu'}\right]. \tag{5}$$

Here, $h\omega^\mu$ is the nuclear transition energy when the ion is in the electronic state $|\mu\rangle$. $W_{\mu\mu'}$ is the transition probability rate for the $|\mu\rangle \rightarrow |\mu'\rangle$ transition between ionic spin states. The amplitude $q_\alpha = a_\alpha + \mathrm{i}b_\alpha$ in equation (4) is calculated from the eigenvectors of **P**:

$$q_\alpha = \sum_{\tau,\mu=1}^{6} N_\mu \Lambda_{\mu\alpha} \Lambda^{-1}_{\alpha\tau} \tag{6}$$

where N_μ is the thermal population of the electronic level μ. $\mathbf{\Lambda}$ is the (6×6) matrix composed of the eigenvectors $\Lambda_{\mu\tau}$ of **P**, i.e.,

$$\mathbf{\Lambda}^{-1}\mathbf{P}\mathbf{\Lambda} = \mathbf{D} \tag{7}$$

where **D** is the diagonal matrix containing the eigenvalues p_α of **P**. The rates of $|5/2\rangle \rightarrow |3/2\rangle$, $|3/2\rangle \rightarrow |1/2\rangle$, and $|1/2\rangle \rightarrow |-1/2\rangle$ flipping between ionic levels due to the spin–spin relaxation are given by 5Ω, 8Ω, and 9Ω, respectively, and the relaxation time (RT) is given by the relation $\mathrm{RT} = [7(1+s)\Omega]^{-1}$. The relative thermal population of the successive Zeeman states of the Fe^{3+} ions is denoted by s.

The Mössbauer spectrum has contributions from A and B sites. As a result, I_1 (as well as I_3) consists of two components. The paramagnetic components in I_3 overlap strongly and, therefore, can be fitted using just one doublet, to a good approximation. Thus, the spectra in zero field are fitted with two sextets and a doublet. In the presence of the applied field of 5 T, superparamagnetic fluctuations are suppressed. Consequently, the paramagnetic component disappears. Thus, Mössbauer spectra in the presence of the field of 5 T are fitted with just two sextets. The relative intensities of the two sextets corresponding to the A and B sites are constrained to the values found from the paramagnetic spectrum (table 1). $H_{int}(0)$, Γ, electric quadrupole shifts, and the relative line intensities of the three pairs of lines in a sextet are obtained by fitting the spectrum at the low temperature where the relaxation broadening is negligible. The relative centre shift of the two sextets is constrained to the value found at 4.2 K. The zero-field spectra at higher temperatures are fitted by treating s and Ω as variable parameters. In fitting the spectra obtained in the magnetic field of 5 T, it is found necessary to treat Γ also as temperature dependent. This is related to the effects of the spin-glass ordering, as discussed later.

Solid lines in figures 4 and 5 show the theoretical spectra which best fit the experimental data. The component theoretical spectra are shown by the dotted lines. We use the least-squares procedure to fit the experimental data. The results of the analyses are given in tables 3 and 4. The temperature dependencies of the relaxation times corresponding to the two sextets, in the presence of the applied field, are shown in figures 6(a) and 6(b). The temperature dependencies of Γ are shown in figures 7(a) and 7(b). The temperature dependencies of $\langle S_z \rangle$ are shown in

Table 3. Results of analyses of Mössbauer spectra obtained in the absence of an applied field. $\epsilon(M) = (\Delta_{12} - \Delta_{56})/4$; $\epsilon(P) = e^2qQ/4$; δ represents the centre shift relative to α-Fe. RT represents the relaxation time. The parameters characterizing the A-site component are: H_{int}(A) = 495 kOe, $\epsilon(M) = -0.013$ mm s^{-1}, I_{16}:I_{25}:I_{34} = 2.8:2.0:1.0, linewidth = 0.38 mm s^{-1} for all lines. The parameters characterizing the B-site component are: H_{int}(B) = 500 kOe, $\epsilon(M) = -0.001$ mm s^{-1}, I_{16}:I_{25}:I_{34} = 3.0:2.0:1.0, linewidth = 0.38 mm s^{-1} for all lines.

Temperature	Component 1 A site		Component 2 B site		Component 3		
(K)	$\langle S_z \rangle$	RT (ns)	$\langle S_z \rangle$	RT (ns)	$\epsilon(P)$	δ	RI (%)
4.2	1.42	6.07	2.16	4.49			
5.0	1.12	6.63	2.11	4.55			
6.0	0.83	3.51	2.00	4.78	0.63	0.26	2.9
7.0	0.75	2.34	1.92	5.52	0.55	0.23	4.76
8.0	0.71	1.89	1.85	5.94	0.52	0.24	6.54
9.0	0.62	1.17	1.64	6.80	0.52	0.26	14.52
10.0	0.45	0.77	1.47	7.35	0.52	0.26	18.7
12.0	0.11	0.37	1.17	13.36	0.51	0.28	18.7
14.0	0.0	0.35	1.17	17.14	0.53	0.28	37.1
15.0	0.0	0.18	1.32	—	0.49	0.28	52.15
20.0	0.0	0.06	1.75	—	0.46	0.27	76.8

Table 4. Results of analyses of Mössbauer spectra obtained in the presence of an applied field of 5 T. $\epsilon(M) = (\Delta_{12} - \Delta_{56})/4$; $\epsilon(P) = e^2qQ/4$; δ represents the centre shift relative to α-Fe. RT represents the relaxation time. The parameters characterizing the A-site component are: H_{int}(A) = 495 kOe, $\epsilon(M) = -0.015$ mm s^{-1}, I_{16}:I_{25}:I_{34} = 2.84:1.53:1.0. The parameters characterizing the B-site component are: H_{int}(B) = 500 kOe, $\epsilon(M) = -0.001$ mm s^{-1}, I_{16}:I_{25}:I_{34} = 2.84:1.53:1.0.

Temperature	Component 1 A site		Component 2 B site	
(K)	$\langle S_z \rangle$	RT (ns)	$\langle S_z \rangle$	RT (ns)
4.2	1.96	2.84	2.255	4.85
5.0	1.88	2.46	2.237	4.33
6.0	1.75	2.37	2.195	3.00
8.0	1.44	1.56	2.08	2.82
9.0	1.39	1.24	2.06	1.70
12.0	1.11	0.84	1.96	1.41
15.0	0.91	0.61	1.885	1.21
40.0	0.27	0.02	1.60	0.92

figure 8. The paramagnetic component is absent in the spectra in the applied field, showing that the superparamagnetic effects are absent. Thus, the increase in the relaxation time at low temperatures is related to the freezing of spins only.

3. Discussion

3.1. Magnetic behaviour of mixed ferrites

Ferrites in which a proportion of the magnetic ions are replaced by diamagnetic cations are known as mixed ferrites. As a result of the substitution for the magnetic ions on one of the sublattices with diamagnetic cations, spins on the neighbouring sublattice become

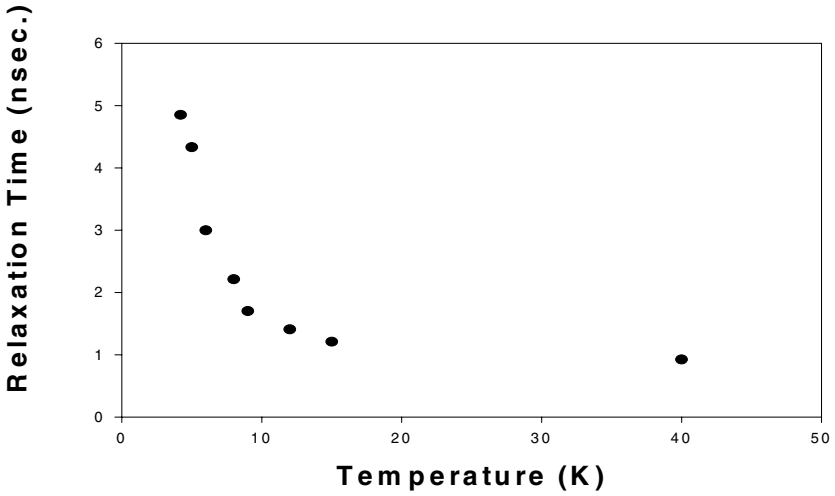

(a)

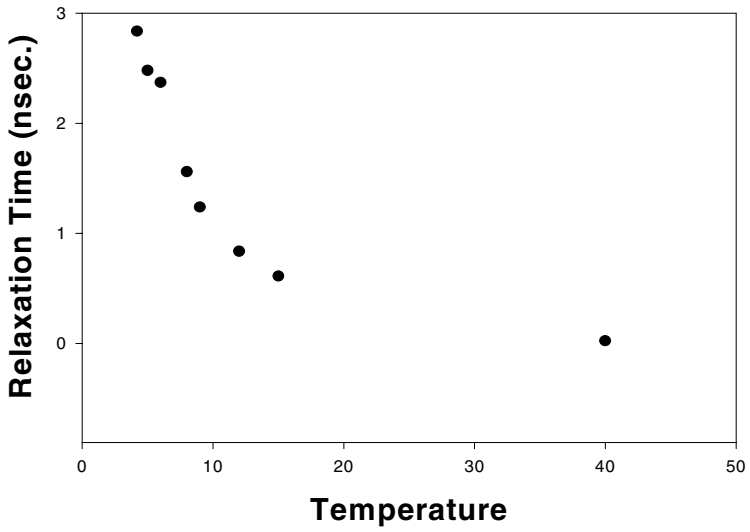

(b)

Figure 6. (a), (b) The temperature dependencies of the relaxation times characterizing the component spectra in the Mössbauer spectrum of $MgAl_{1.4}Fe_{0.6}O_4$, in the presence of an applied magnetic field of 5 T.

non-collinear with the net magnetization. This occurs when the inter-sublattice interaction becomes weaker than the intra-sublattice interaction, as a result of the substitution. There are two magnetic transition temperatures [2, 12]. At the lower transition temperature, denoted by T_{YK}, the non-collinearity appears on lowering the temperature. At the higher transition temperature, T_P, paramagnetic ordering changes into a collinear ferrimagnetic ordering on lowering the temperature. As is well known, two transition temperatures are defined in the discussion of the ordering in the re-entrant spin glasses [16–19] also, which are related to the two transitions described above. Such an oxide shows a kink in the temperature dependence of $\langle S_Z \rangle$, as described earlier. At larger concentrations of the diamagnetic cations, we expect a

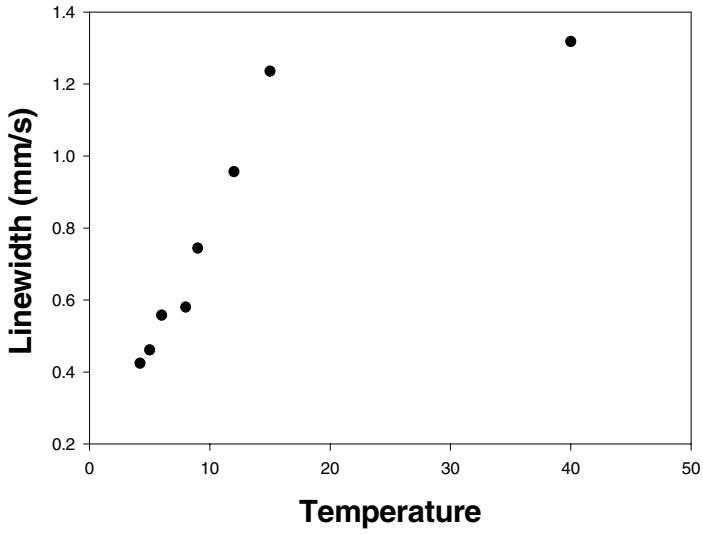

(a)

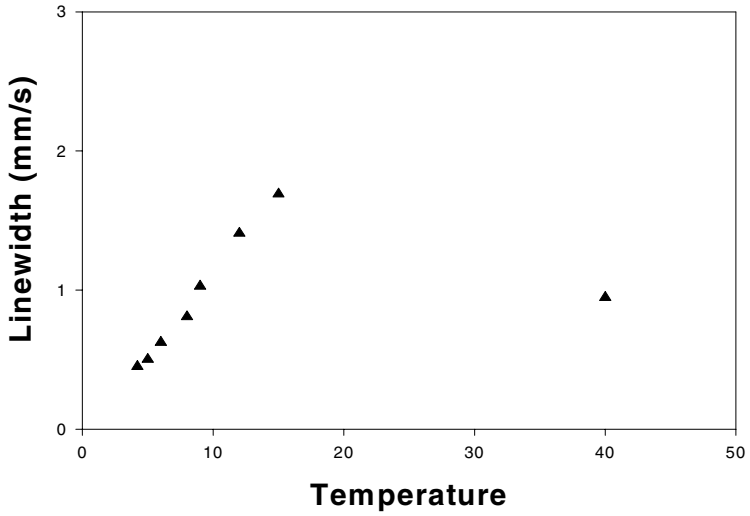

(b)

Figure 7. (a), (b) The temperature dependencies of the linewidths (Γ_{16} and Γ_{25}) characterizing the component spectra in the Mössbauer spectrum of $MgAl_{1.4}Fe_{0.6}O_4$ in the presence of an applied magnetic field of 5 T. Γs exclude the broadening due to the single ion relaxation effect. The widths of the corresponding lines in the two component spectra are assumed to be equal.

transition directly from a paramagnetic state to a spin-glass state. The present measurements show that $MgAl_{1.4}Fe_{0.6}O_4$ belongs to this category.

3.2. AC susceptibility

The rapid decrease in the AC susceptibility, the response to an applied field, at temperatures below the cusp temperature (figure 1) indicates that the response of the Fe moments is being increasingly hindered as the temperature lowers, in agreement with the temperature dependence

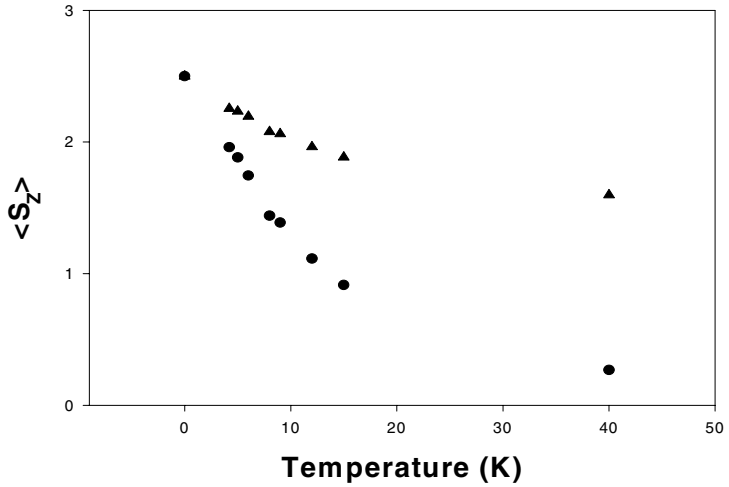

Figure 8. The temperature dependencies of $\langle S_Z \rangle$ characterizing the component spectra in the Mössbauer spectrum of $MgAl_{1.4}Fe_{0.6}O_4$ in the presence of an applied magnetic field of 5 T.

of the relaxation time found using Mössbauer spectroscopy (figure 6). Considerable irreversibility and the time-dependent effects which appear at temperatures below T_{sg} in canonical metallic spin glasses [16–19] have led to an explanation in terms of the thermal activation over the potential energy barriers with a broad distribution of barrier heights. There are a large number of nearly degenerate spin configurations presumably separated by energy barriers. In the mixed oxide under study also, spin configurations in different clusters are different and weakly related. As a result, there are a large number of spin configurations, separated by barriers, into which the system can settle on lowering the temperature [2]. There is, thus, a resemblance between the conditions found in the oxide under study and those in a canonical spin glass at low temperatures. The anomaly in the susceptibility is caused by the sharp increase in the relaxation time as the system settles into one of these configurations on lowering the temperature.

The peak in the AC susceptibility (figure 1) occurs at a temperature higher than the range of temperatures where superparamagnetic effects are shown by the Mössbauer spectroscopy (figure 4). Thus, the peak cannot be due to superparamagnetism, but is due to the spin-glass ordering. The divergence in the non-linear susceptibility also shows that the peak is not due to superparamagnetism, but due to a thermodynamic phase transition to a spin-glass state. The peak in the susceptibility at T_{sg} decreases and moves to lower temperatures as the field increases (figure 1). This is similar to the behaviour found for a canonical spin glass. θ/T_{sg} is found to be large and shows the presence of strong frustration. This is responsible [41] for the spin-glass ordering shown by the oxide.

We see another transition at 136 K. $\chi_0^t(M)$ shows a very weak shoulder at this transition, which gets easily suppressed by the DC field (figure 1). $\chi_2^t(M_3)$ shows a broad and prominent peak at 136 K (figure 2), while $\chi_4^t(M_5)$ shows a weak peak at this temperature (figure 2). Mössbauer spectroscopy, on the other hand, does not show any long-range magnetic ordering at these temperatures. We, therefore, believe that this peak in χ_2^t is related to the development of short-range order as the temperature approaches T_{sg}. The temperature dependence of the susceptibility according to the Curie–Weiss law is

$$\chi = \frac{C}{T - \theta} \tag{8}$$

where $C = N\mu^2$. Due to the increase in the short-range order [21, 22], μ increases and N decreases as the temperature is lowered. However, unlike for other spin glasses, C saturates at lower temperatures in the oxide under study. This is because the magnetic lattice in the oxide is composed of clusters. The short-range order in a cluster cannot involve ions in other clusters. This saturates C and results in a hump in the susceptibility.

In metallic spin glasses, the magnetic interactions are due to the RKKY interactions. In view of the long-range nature of this interaction, the mean-field theories in which an ion interacts with all of the magnetic ions in the lattice are appropriate. In metallic systems, the competing interactions can be represented by a Gaussian distribution, with first and second moments denoted by J_0 and J, respectively. In a system with $J_0 > J$, a ferromagnetic ground state evolves [45] below $T_P \propto J_0$. In the opposite limit, $J_0 < J$, a phase transition still occurs at $T_{sg} \propto J$, but to a spin-glass state. Above T_{sg}, χ_{nl} is given by

$$\chi_{nl} = \chi(0,t) - \chi(h,t) = t^{\beta} F\left(\frac{h^2}{t^{\gamma+\beta}}\right) \approx h^2 t^{-\gamma} - h^4 t^{-(2\gamma'+\beta')}. \tag{9}$$

The effective-field model and the experimental observations show a symmetric behaviour of χ_{nl} around T_{sg}. Between these two limits ($J_0 > J$ and $J > J_0$), there exists a rather interesting regime in which the paramagnetic-to-ferromagnetic transition is followed by one or more subsequent transitions, in which one or more spin components undergo spin freezing. From the AC susceptibility, this sequence is identified with the occurrence of a rapid increase in the response with decreasing temperature as the ferromagnetic phase is approached from above, an intermediate plateau-like region, followed by an abrupt decrease at lower temperature, signifying the entry into a spin-glass phase. Remarkably, in the case of FeZr, the lower temperature at which χ_{nl} shows an anomaly has been found to coincide with the temperature T_{YK} at which the non-collinearity develops, as found using Mössbauer spectroscopy [45, 46]. This supports our belief that the two transition temperatures for the mixed ferrites mentioned above (T_P and T_{YK}) correspond to T_P and T_{sg} for re-entrant spin glasses.

We observe a strong peak in χ_{nl} at T_{sg}. The critical exponents are found to be $\gamma = 1.47$ and $\beta = 0.54$. In earlier studies, γ has been found to vary [30, 31] from material to material in the range from 1.2 to 3.6. There are also differences between the exponent values predicted by the mean-field approaches [47, 48] ($\gamma = 1, \beta = 1, \delta = 2$), the short-range Ising models [49–50], and the Heisenberg models ($\gamma = 2.9 \pm 0.3, \beta \approx 0.50$). This result may mean that not all spin glasses belong to one universal class. The presence of finite-temperature phase transitions in them is, however, well supported by the experiments. Fahnle and Souletie [51] have argued that the material-dependent γ for spin glasses might not be a true critical exponent.

3.3. Mössbauer spectra

In view of the random nature of the distribution of the cations (Fe, Al, and Mg) on the two sublattices, and the large population of diamagnetic cations at the two sites, the magnetic ordering cannot be antiferromagnetic. We consider the effect of a longitudinal (parallel to the direction of the γ-rays) field on a ferrimagnetically ordered (collinear or non-collinear) magnetic substance. The applied field aligns the magnetic domains parallel to it. There are two ways in which the Mössbauer spectrum is affected. Firstly, the relative intensities of the second and the fifth lines in the sextet change. The relative intensities are [12, 13]

$$I_{16}{:}I_{25}{:}I_{34} = 3(1+\cos^2\alpha){:}4\sin^2\alpha{:}(1+\cos^2\alpha) \tag{10}$$

where α is the orientation of the spin relative to the direction of the γ-rays. Thus, the relative intensities of the three pairs of lines of the sextet change from 3:2:1 to 3:0:1 if $\alpha = 0$ or 3:4:1 if $\alpha = 90^\circ$ when a longitudinal magnetic field is applied. Secondly, the subspectra corresponding

to the A and B sublattices of the ferrite split. The effective field (H_{eff}) in the presence of an applied field (H_{app}) is given by [12, 13]

$$H_{eff} = [H_{int}^2 + H_{app}^2 + 2H_{int}H_{app}\cos\alpha]^{1/2}. \tag{11}$$

Here, H_{int} represents the hyperfine field in the absence of the applied field. When the A and B sublattices are anti-parallel, $\boldsymbol{H}_{eff}$(A) and $\boldsymbol{H}_{eff}$(B) change in opposite directions. As a result, the component spectra corresponding to the A and B sublattices split.

If the relative intensities do not change on the application of $\boldsymbol{H}_{app}$, the non-collinearity angle can be 54.7°. But in this case, H_{int} will change significantly and the subspectra corresponding to the A and B sites will split. On the other hand, when H_{int} does not change on the application of $\boldsymbol{H}_{app}$, the angle is ≈90°, but in this case the RI of the three pairs of lines should change from 3:2:1 to 3:4:1. If the relative intensities of the three pairs of lines do not change and the spectrum does not split into component spectra, as is found in the present study, the presence of a spin-glass ordering which is not affected by $\boldsymbol{H}_{app}$ is unambiguously shown.

In earlier studies of the mixed ferrites, it has been possible to interpret the Mössbauer spectra, in the absence as well as in the presence of an applied magnetic field, very satisfactorily using the stochastic model of single-ion spin relaxation. This could be done by treating only $\langle S_z \rangle$ and the relaxation time as temperature-dependent parameters. Γ was found to be temperature independent. In the present study, we expect to see additional static as well as dynamic effects of the spin-glass ordering. The analyses show that the zero-field spectra do not exhibit additional features. This is due to the microscopic nature of the Mössbauer probe. As a result, the spin of the parent ion alone is responsible for the hyperfine field and the directions of the neighbouring ions are not important. In the presence of the applied field, however, effects of the spin-glass ordering are found. The analyses showed that Γ has a temperature-dependent contribution. Both static and dynamic effects of the spin-glass ordering can be responsible for this. The application of a large external field can induce alignment of spins in a spin-glass oxide. As A- and B-site spins are ferrimagnetically oriented, the sublattice with larger magnetization tends to orient parallel to $\boldsymbol{H}_{app}$ and the other sublattice anti-parallel to it. This alignment increases with temperature. This is implied by the increase in susceptibility with temperature as the temperature approaches T_{sg}. The induced alignment increases Γ with temperature. The decrease in the relative intensities of the second and fifth lines as a result of the application of the external field is also due to this induced alignment in the spin-glass oxide. The effect is, however, small and does not split A- and B-site spectra. The dynamical freezing of spins as a result of the spin-glass ordering is also responsible for the temperature-dependent contribution to Γ. When the fluctuation rate is small, the effect is an increase in the linewidth only. When the fluctuation rate is large, the effect is not only an increase in the linewidth but also shifts of the line positions towards the centre of the spectrum. At T_{sg}, the fluctuations among the different configurations in which the system can occur is rapid. This not only broadens the lines but also causes movement of the lines towards the centre. As the temperature is lowered, the fluctuation rate reduces (spin freezing) and one of the configurations gets preferentially populated. In this case, the effect of fluctuations is to increase the linewidth only. This, thus, gives a temperature-dependent contribution to Γ which decreases with temperature, as is experimentally observed.

4. Conclusions

Spin-glass ordering is seen in a cubic spinel ferrite for the first time. This is shown by a peak in the AC susceptibility. The application of a DC field suppresses the peak and shifts it to lower temperatures, as is found for metallic spin glasses. χ_{nl} confirms the presence of

a thermodynamic phase transition at T_{sg}. The critical exponents estimated ($\gamma = 1.47$ and $\beta = 0.54$) fall in the range found using other spin glasses. Mössbauer measurements in zero field do not give any indication of the spin-glass ordering. However, spectra taken in strong applied fields show characteristics that can be used to identify the presence of spin-glass ordering in other oxides.

Acknowledgments

Partial financial support was provided by the Natural Sciences and Engineering Research Council of Canada. One of the authors (SCB) is indebted to Professor R M Roshko for many discussions and Professor Gwyn Williams for clarifying the role of the remanant field in giving finite even-harmonic terms.

References

[1] Bhargava S C and Iyengar P K 1971 *Phys. Status Solidi* b **46** 117
Bhargava S C and Iyengar P K 1972 *Phys. Status Solidi* b **53** 359
[2] Bhargava S C 1998 *Phys. Rev.* B **58** 3240
[3] Bhargava S C and Zeman N 1980 *Phys. Rev.* B **21** 1717
[4] Bhargava S C and Iyengar P K 1974 *J. Physique Coll.* **35** C6 669
[5] Bhargava S C, Morup S and Knudsen J E 1976 *J. Physique Coll.* **37** C6 93
[6] Bhargava S C, Mulder F M, Thiel R C and Kulshreshtha S K 1980 *Hyperfine Interact.* **54** 459
[7] Dormann J L, Bhargava S C, Jove J and Fiorani D 1989 *Hyperfine Interact.* **50** 625
[8] Yafet Y and Kittel C 1952 *Phys. Rev.* **87** 290
[9] Lotgering F K 1956 *Phillips Res. Rep.* **11** 190
[10] Rosencwaig A 1970 *Can. J. Phys.* **48** 2857
Rosencwaig A 1970 *Can. J. Phys.* **48** 2868
[11] Daniels J M and Rosencwaig A 1970 *Can. J. Phys.* **48** 381
[12] Bhargava S C and Zeman N 1980 *Phys. Rev.* B **21** 1726
[13] Sundararajana M D, Narayanasamy A, Nagarajan T, Haggstrom L, Swamy C S and Ramanujachary K V 1984 *J. Phys. C: Solid State Phys.* **17** 2953
[14] Morrish A H and Clark P E 1975 *Phys. Rev.* B **11** 278
[15] Piekoszewski J, Dabrowski L, Suwalski J and Makolagwa S 1977 *Phys. Status Solidi* a **39** 643
[16] Binder K and Young A P 1986 *Rev. Mod. Phys.* **58** 801
[17] Williams G 1987 *Can. J. Phys.* **65** 1251
[18] Chowdhury D 1986 *Spin Glasses and Other Frustrated Systems* (Singapore: World Scientific)
[19] Fiorani D 1988 *The Time Domain in Surface and Structural Dynamics* ed J Long and F Grandjean (New York: Academic)
[20] Zastre E, Roshko R M and Williams G 1985 *Phys. Rev.* B **11** 7597
[21] Morgownik A F J and Mydosh J A 1981 *Phys. Rev.* B **24** 5277
[22] Alba M, Hammann J and Nogues M 1982 *J. Phys. C: Solid State Phys.* **15** 5441
[23] Singh M R and Bhargava S C 1994 *Solid State Commun.* **90** 183
[24] Singh M R and Bhargava S C 1995 *Solid State Phys. (India)* C **38** 139
[25] Singh M R and Bhargava S C 1995 *J. Phys.: Condens. Matter* **7** 8183
[26] Levy L P 1988 *Phys. Rev.* B **38** 4963
[27] Suzuki M 1977 *Prog. Theor. Phys.* **58** 1151
[28] Chalupa J 1977 *Solid State Commun.* **22** 315
[29] Taniguchi T, Miyako Y and Tholence J L 1985 *J. Phys. Soc. Japan* **54** 220
[30] Kunkel H P and Williams G 1988 *J. Magn. Magn. Mater.* **75** 98
[31] Tobo A and Ito A 1998 *J. Phys. Soc. Japan* **67** 297
[32] Villain J 1979 *Z. Phys.* B **33** 31
[33] Dormann J L and Nogues M 1990 *J. Phys.: Condens. Matter* **2** 1223
[34] Poole C P Jr and Farach H A 1982 *Z. Phys.* B **47** 55
[35] Scholl F and Binder K 1980 *Z. Phys.* B **39** 239
[36] Bhargava S C 1986 *J. Phys. C: Solid State Phys.* **19** 7045

[37] Dormann J L, El Harfaoui M, Nogues M and Jove J 1987 *J. Phys. C: Solid State Phys.* **20** L161
[38] Brand R A, Georges-Gilbert H, Hubsch J and Heller J A 1985 *J. Phys. F: Met. Phys.* **15** 1987
[39] De Grave E, Govaert A, Chambaere D and Robbrecht G 1979 *Physica* B **96** 103
[40] de Bakker P M A, Vandenberghe R E and de Grave E 1997 *J. Physique Coll.* IV **7** C1 267
[41] Ramirez A 1991 *J. Appl. Phys.* **70** 5952
[42] Clauser M J 1971 *Phys. Rev.* B **11** 3748
[43] Bhargava S C, Knudsen J E and Morup S 1979 *J. Phys. C: Solid State Phys.* **12** 2879
[44] Bhargava S C 1983 *Advances in Mossbauer Spectroscopy* ed B V Thosar, P K Iyengar, J K Srivastava and S C Bhargava (Amsterdam: Elsevier)
[45] Ma H, Kunkel H P and Williams G 1991 *J. Phys.: Condens. Matter* **3** 5563
[46] Ryan D H, Ström-Olsen J O, Provencher R and Townsend M 1988 *J. Appl. Phys.* **64** 5787
[47] Sherrington D and Kirkpatrick S 1975 *Phys. Rev. Lett.* **35** 1972
[48] Kirkpatrick S and Sherrington D 1978 *Phys. Rev.* **17** 4384
[49] Ogielski A T 1985 *Phys. Rev.* B **32** 7384
[50] Young A P and Bhatt R N 1986 *J. Magn. Magn. Mater.* **54–57** 6
[51] Fahnle M and Souletie J 1984 *J. Phys. C: Solid State Phys.* **17** L469